Published in final edited form as:

J Alzheimers Dis. 2016 April 8; 52(4): 1263–1275. doi:10.3233/JAD-160033.

Transthyretin Suppresses Amyloid-β secretion by Interfering with Processing of The Amyloid-β Precursor Protein

Xinyi Li[1], **Yuanli Song**[2], **Charles R. Sanders**[2], and **Joel N. Buxbaum**[1]

Jassen Research & Development, LLC, Johnson & Johnson, 3210 Merryfield Rd, San Diego, CA 92121

Bristol-Myers Squibb, Biologics Process Development, 38 Jackson Rd., Devens, MA 01434

[1]The Scripps Research Institute; Department of Molecular and Experimental Medicine, 10550 North Torrey Pines Road, La Jolla, CA 92037

[2]Vanderbilt University School of Medicine, Department of Biochemistry and Center for Structural Biology, Nashville, Nashville, TN 37232-8725

Abstract

In Alzheimer's disease (AD) most hippocampal and cortical neurons show increased staining with anti-transthyretin (TTR) antibodies. Genetically programmed over-expression of wild type human *TTR* suppressed the neuropathologic and behavioral abnormalities in APP23 AD model mice and TTR-Aβ complexes have been isolated from some human AD brains and those of APP23 transgenic mice. In the present study *in vitro* NMR analysis showed interaction between the hydrophobic thyroxine binding pocket of TTR and the cytoplasmic loop of the C99 fragment released by β-secretase cleavage of AβPP with K_d = 86±9 μM. In cultured cells expressing both proteins the interaction reduced phosphorylation of C99 (at T668) and suppressed its cleavage by γ-secretase significantly decreasing Aβ secretion. Coupled with its previously demonstrated capacity to inhibit Aβ aggregation (with the resultant cytotoxicity in tissue culture) and its regulation by HSF1 these findings indicate that TTR can behave as a stress responsive multimodal suppressor of AD pathogenesis.

Keywords

Alzheimer's disease; transthyretin; phosphorylation; gamma secretase; Aβ; AβPP; APP; APP23; Nuclear magnetic resonance

The majority of neurons in the brains of patients with Alzheimer's disease (AD) stain with antibodies specific for the protein transthyretin (TTR) a systemic amyloid precursor [1–3]. Similarly immunohistochemistry of the brains in transgenic murine models of human Aβ deposition show diffuse TTR staining in cortical and hippocampal neurons and focal staining of plaques and vessels [2,3]. Studies in our laboratory demonstrated that the positive TTR staining reflected neuronal TTR synthesis rather than uptake of TTR released from the

*Correspondence to: Joel N. Buxbaum, M.D., The Scripps Research Institute, Department of Molecular and Experimental Medicine, Room 230, La Jolla, CA 92037, USA. Tel.:+1 858 784 8885; Fax: +1 858 784 8891; jbux@scripps.edu.

choroid plexus and that neuronal *TTR* gene expression was regulated in a stress responsive manner by the transcription factor heat shock factor 1 (HSF1) [3,4]. A beneficial function of neuronal TTR *in vivo* was strongly indicated in the APP23 murine model of human Aβ deposition in which mice bearing a multi-copy construct of a wild type human TTR (wt h*TTR*) gene with tissue specific overexpression had substantially reduced neuropathologic and behavioral manifestations of Aβ deposition [5]. Consistent with those studies is the earlier observation in the Tg2576 transgenic AD model that unilateral intraventricular injection of an anti-TTR antibody increased ipsilateral Aβ deposition when compared with the opposite hemisphere and the more recent demonstration that co-injection of TTR reduces the AD like pathology induced in a rodent model in which preformed oligomeric Aβ1-42 complexes are injected intracerebrally [6,7]. Independent reports from two laboratories indicated that the pathology evident in different transgenic models of human Aβ deposition is accelerated in the absence of one or both copies of the endogenous murine *Ttr* gene, although this finding has not been seen in laboratories using very aggressive models of Aβ deposition and/or experimental protocols less sensitive to the rate of Aβ deposition [5,8–10]. In the aggregate these observations suggest that TTR, despite being a systemic amyloid precursor, is involved in neuronal resistance to the neuropathology produced by amyloidogenic Aβ aggregation.

There is substantial *in vitro* evidence showing that TTR inhibits the aggregation of $A\beta_{1\text{-}40/42}$ monomers required to form toxic oligomers, a notion consistent with the isolation of TTR-Aβ complexes from the brains of APP23 model mice and some human AD subjects [3]. Multiple experiments from many laboratories have described interaction of TTR with Aβ monomers and oligomers resulting in inhibition of oligomerization and fibril formation as well as reduced toxicity for a variety of cultured cell targets [11–17]. In addition it has been observed that TTR will inhibit the toxicity of preformed toxic oligomers by fostering oligomeric growth in such a way as to render the oligomers non-toxic [18], a property that appears to be shared with molecules classified as extracellular chaperones [19].

Aβ is released by γ-secretase cleavage from its immediate precursor, the transmembrane 99 residue C-terminal fragment of AβPP, C99 (also known as β-CTF, reviewed in [20]). In our earlier studies of brains from APP23 transgenic mice over-expressing wt h*TTR* we found that while the amount of C99 was comparable to that in mice without the human TTR construct, the proportion remaining in the soluble fraction of the extract was much greater in the presence of TTR. Further, there was a marked reduction in the concentration of SDS and formic acid extractable $A\beta_{1\text{-}40}$ and $A\beta_{1\text{-}42}$ [5]. This observation suggested either that clearance of Aβ, presumably as TTR-Aβ complexes, was very efficient, or that in addition to binding Aβ, TTR also interfered with the cleavages necessary for its production or secretion. We now report the results of *in vitro*, cell culture, and *in vivo* experiments designed to determine whether, in addition to suppressing Aβ oligomerization and detoxifying the aggregates, TTR also suppresses formation of the amyloidogenic Aβ fragments thus posing the question, does TTR have multiple mechanisms active in protecting neurons from the effects of Aβ aggregates?

MATERIALS AND METHODS

NMR titrations of TTR and C99 and related analysis

The 99 residue C-terminal fragment of the human amyloid precursor protein, C99, was expressed and purified into micelles of the mild lipid-derived detergent lyso-myristoyl-phosphatidylglycerol (LMPG, Anatrace, Maumee, OH) [21]. Human TTR was expressed and purified as previously described [16]. Following purification the LMPG concentration was adjusted to 5% (percentage by weight), the pH was adjusted to 7.2, and the ^{15}N-labeled C99 concentration was adjusted to 0.25 mM in low or high salt conditions. TTR was buffer exchanged to 20 mM NaH_2PO_4 (low salt condition) or 100 mM NaH_2PO_4 (high salt condition) at pH 7.2 with a PD-10 column (GE Healthcare) and was concentrated to 1.6 mM, followed by addition of LMPG to 5%. Using low salt conditions, TTR was titrated into ^{15}N-labeled C99 to concentrations of 0.10, 0.20, 0.40, and 0.80 mM. Under high salt conditions, TTR was titrated into ^{15}N-labeled C99 to the concentrations of 0.03, 0.10, 0.20, 0.40, and 0.80 mM. The reverse titration was conducted by titrating 2 mM C99 to a solution containing 0.10 mM ^{15}N labeled TTR under the pH 7.2 high salt condition All solutions contained 5% LMPG.

For each titration point a 2-D ^{15}N-^{1}H TROSY NMR spectra was acquired at 310K using a 900 MHz Bruker spectrometer (Figure 1). Peak assignments for ^{15}N-labeled C99 and TTR were obtained from previous work [16,22]. The chemical shifts for peaks that exhibited relatively large chemical-induced shifts were plotted as a function of the concentrations of the unlabeled protein being added. Using Origin 8.0 (OriginLab Corp. Northampton, MA) the data were fit to a single binding site model with the equation of $y=x*B_{max}/(K_d+x)$, where y is the absolute value of the change in chemical shift (relative to the condition without ligand), x is the concentration of the added unlabeled protein, Bmax is the maximum change in chemical shift observed for a given resonance upon the saturation of binding by the titrating protein, and K_d is the dissociation constant.

Cell culture and transfection

7PA2 and 7WD10 cells were kindly provided by Prof. E. Koo (University of California, San Diego). 7PA2 is a Chinese hamster ovary (CHO) cell line stably expressing the $APP_{Val717Phe}$ familial APP mutation, while 7WD10 cells are CHO-derived and stably express wt human AβPP [23]. 7PA2 and 7WD10 cells were cultured in Dulbecco's modified Eagle's medium (DMEM) with 10% fetal bovine serum (FBS), 1% penicillin/streptomycin, 2mM L-glutamine, and G418 (200 μg/ml) (Invitrogen). SH-SY5Y human neuroblastoma cells were cultured in 1:1 mixture of DMEM: F12 medium with the same supplement minus G418 (Invitrogen).

Transfections—pcDNA-TTR was constructed using the pcDNA4.0 vector (Life technologies). TTR cDNA with and without its leader sequence was cloned in the same vector. pcDNA-lacZ was used as a transfection control in all experiments. The CHO cells were transfected using X-tremeGENE 9 DNA Transfection Reagent (Roche) and SH-SY5Y cells were transfected with the CalPho Mammalian Transfection Kit (Clontech Laboratories). After CalPho transfection, the media were replaced the next day. To evaluate

the sAPP's, the cells in 6-well plates were washed with PBS, and cultured in 600 μl of DMEM without phenol or serum for 2 days when the media were collected for analysis.

Secretase inhibitors

N-[(3,5-Difluorophenyl)acetyl]-L-alanyl-2-phenyl]glycine-1,1-dimethylethyl ester (DAPT) 1 μM (Tocris) was used to inhibit γ-secretase and accumulate AβPP C-terminal fragments (C99), while 1.5μM β-Secretase Inhibitor IV (EMD Millipore) was used to inhibit β-secretase.

Aβ ELISA

The cells were cultured on 96-well plates (Corning) overnight then transfected with pcDNA-TTR or control plasmid. The culture medium was collected after 24 hours. The medium was analyzed by an Aβ ELISA as follows. Monoclonal 6E10 anti-Aβ(residues 1–17) mouse IgG1, (Biolegend) was coated in 50 mm carbonate buffer, pH 9.6, at 4°C overnight on high binding assay black plates (Costar), washed with TBST (tris buffered saline with 0.05% Tween 20) and blocked with 5% non-fat milk in TBST. Samples and standards (synthetic $A\beta_{1\text{-}40}$) were incubated for 2 hr, followed by addition of biotin-labeled 4G8 [anti-Aβ residues 17–24, mouse IgG2b (Biolegend)] and incubation for 1 hr at 37°C. After washing, streptavidin horseradish peroxidase (HRP) conjugate (Invitrogen) was added and incubated for 45 min, followed by detection by Quanta Blue fluorogenic peroxidase substrate (Thermo Scientific) using a Tecan Safire II fluorescence plate reader.

Co-immunoprecipitation

DAKO anti-TTR antibody (DAKO) was cross-linked to Dynabeads (Life technologies) as previously described using the manufacturer's protocol [3]. Cells were seeded in 10 cm dishes and transfected with pcDNA-TTR or control plasmid then treated with DAPT. After 24hr incubation, the cells were scraped from the plates, collected and washed twice using PBS by centrifugation at 200g at 4°C. The cells were re-suspended in 1 ml PBS, then incubated with 0.5 mM cell permeable cross-linking reagent DSP (Dithiobis[succinimidyl propionate]) (Thermo Scientific) for 30 min at room temperature. The cells were collected by centrifugation, resuspended in lysis buffer (50 mm Tris, pH 7.5, 150 mm NaCl, 3 mm EDTA, 1% Triton X-100) supplemented with complete mini protease inhibitor mixture (Roche) and phosphatase inhibitor cocktail tablets PhoSTOP (Roche) on ice for 1 hr. The lysates were centrifuged at 10,000g for 10 min at 4°C. The supernatants were incubated with antibody cross-linked beads at room temperature for 30 min, eluted by 20 μl of 0.2 M glycine pH 2.6 for 10 min. Eluates were neutralized with 3 M tris pH 8.5 and analyzed by western blotting.

Digitonin extraction

Cells were washed with PBS, collected by centrifugation at 200g at 4°C then re-suspended in HEPES buffer (20 mM cold HEPES, 100 mM NaCl, 1 mM EDTA, pH 7.5) on ice with 0, 0.005, 0.01, 0.05, 0.1, or 0.25 % of digitonin (Calbiochem), incubated for 30 min then centrifuged at 10,000g for 10 min. The pellets were resuspended in HEPES buffer with 1 % Triton X100, incubated for 10 min on ice then centrifuged at 14,000g for 10 min [24–26].

The digitonin soluble and pellet fractions were analyzed by western blotting probing for the endoplasmic reticulum (ER) marker GRP78 (BIP) (Santa Cruz Biotechnology) and the cytoplasmic marker actin (Sigma-Aldrich).

Western blotting

Samples were electrophoresed in 15 % SDS tris-glycine PAGE and then transferred to PVDF membranes (Biorad). The blots were blocked in 5 % nonfat milk in TBST and then incubated with primary antibodies specific for the protein of interest. The following primary antibodies used were: monoclonal C1/6.1 anti-APP C-terminal fragment (676–695 of APP695), mouse IgG1 (Biolegend), polyclonal anti phospho-APP (Thr668) (Cell Signaling), anti-APP N-terminal 22C11, mouse IgG1 (Millipore), monoclonal 6E10 anti-Aβ residues 1–17, mouse IgG1 (Biolegend), monoclonal anti-actin (Sigma-Aldrich), and polyclonal anti-TTR DAKO (DAKO). The blots were then incubated with IRDye 800CW or IRDye 680-labeled secondary antibodies (LI-COR Bioscience) scanned and quantified with an Odyssey Infrared Imaging system. Raw scan readings were normalized to actin signals from the same sample.

Animal Studies

The brains analyzed were from transgenic and control mice from experiments carried out in compliance with guidelines for animal experimentation and approved by the TSRI Institutional animal care and use committee [5].

RESULTS

Does TTR interact with C99 *in vitro* and what is the interaction interface?

In order to examine whether TTR was intrinsically capable of interacting with C99 in a purified system we conducted nuclear magnetic resonance (NMR) studies in which uniformly ^{15}N-labeled labeled recombinant C99 maintained in a model membrane environment was incubated with recombinant wild type human TTR tetramers under low salt conditions (20 mM sodium phosphate, pH 7.2) [21,27]. We observed TTR-induced resonance shifts for several APP (C99) ^{1}H,^{1}5N-TROSY NMR peaks, including those from residues G659 (734 in APP_{770} numbering), A665 (740) and T668 (743), all located in the cytoplasmic domain of C99 (Fig.1). The TTR concentration-dependence of the changes in peak position for the three sites in each case fit well to a 1:1 binding model (Fig. 1), leading to K_d values that were the same within the range of experimental error: 252±64, 280±55 and 384±86 μM, for G659, A665 and T668 respectively (average K_d = 310±190 μM). These results suggest that TTR binds to C99 in the segment consisting of residues 659-668 (734-743 APP_{770} numbering) located in the cytosolic loop that connects the C99 transmembrane domain to a membrane surface-associated amphipathic helix located at the extreme C-terminus of the protein.

To confirm the interaction under more physiologic conditions we repeated the titration in the presence of a higher salt concentration (100 mM phosphate, pH 7.2). The same C99 NMR peaks shifted in response to increasing TTR, with the data still fitting a 1:1 binding model, but with more avid binding than under the lower salt conditions (K_d = 86±9 μM).

Observation of tighter binding at higher ionic strength indicates that the interaction between C99 and TTR is unlikely to be electrostatically driven, and is more likely to involve hydrophobic interactions.

To verify direct interaction between C99 and TTR and to probe the location of the C99 binding site within TTR we carried out a reciprocal titration where soluble ^{15}N-labeled TTR (provided by Dr. Xin Zhang, Department of Chemistry, The Scripps Research Institute) in the presence of model membranes was titrated with C99 and followed by NMR under physiological salt conditions. A number of TTR peaks were observed to shift in response to increasing C99 concentrations (Figure 2). Fitting of the data again confirmed 1:1 binding between these proteins, with a K_d of 76±20 μM, within the error of the K_d observed in the reciprocal titration described above. Because the NMR spectrum of TTR has previously been assigned under similar conditions to those used in this work we were able to assign most of the peaks exhibiting the greatest shifts in response to binding C99 [28]. These included the assigned peaks for residues L12, M13, V14, V16, R104, and V123. These sites are known to be located in or near the T4/small molecule binding pocket of the TTR tetramer in which the T4 contact residues are E54, K15, A109, L110, S117,T119 [29].

Do TTR and C99 interact in cells engineered to constitutively produce and process AβPP to yield Aβ?

The *in vitro* experiments indicated that purified TTR and C99 form a stoichiometric complex with an affinity of approximately 85 μM. In order to determine whether the interaction was biologically relevant we studied the generation of Aβ in CHO cells expressing AβPP, i.e. 7PA2 (APP751 containing the Val717Phe familial Alzheimer's disease mutation), and 7WD10 (stably expressing a wt human AβPP construct in the same vector) [23], transfected with either a human wild type *TTR* construct or the same vector with the *lacZ* gene substituted for the *TTR* construct. The studies were carried out in the presence or absence of the gamma secretase inhibitor N-[N-(3, 5-Difluoro-phenacetyl-L-alanyl)]-S-phenylglycine *t*-butyl ester (DAPT) which increases the cellular concentration of the C99 fragment by decreasing its proteolytic cleavage [30]. Di-thio-bis [succinimidyl- propionate] (DSP), a membrane permeable cross-linking agent was added to the cells to cross-link interacting proteins prior to cell disruption [31]. The cells were lysed and the cross-linked lysates immunoprecipitated with an anti-TTR antibody covalently bound to magnetic beads. The immune-isolated molecules were analyzed by western blot using anti-TTR and anti-C99 antibodies. These experiments indicated that in the intact cells TTR interacted with both C99 and AβPP (Fig. 3). Re-probing this blot with the anti-pT668 antibody gave no signal, indicating that the interaction was with unphosphorylated forms of APP and C99.

Where do TTR and C99 interact in the cell?

C99 is derived from AβPP by β-secretase (BACE1) cleavage [32]. The fragment persists as a membrane associated protein that undergoes regulated intramembrane proteolysis (RIP) to generate a series of peptides of varying toxic potential [33]. The amino acids implicated by NMR to interact with TTR are in the cytoplasmic loop of the carboxyl domain of C99 [21]. We examined the intracellular distribution of AβPP, C99 and TTR in the transfected cultured 7PA2, 7WD10 and SH-SY5Y human neuroblastoma cells. Differential solubilization of cells

expressing both molecules with increasing concentrations of digitonin showed the three localized predominantly in the endosome-enriched membrane compartment (presumably vesicles), but some TTR and C99 were solubilized by very low digitonin concentrations consistent with a cytoplasmic location (Figure 4) [34]. In the low digitonin "cytoplasmic" fractions two TTR bands were identified, corresponding to the precursor protein with an intact hydrophobic "leader" sequence and the smaller fully processed protein. The ratio of soluble to insoluble fractions of the larger protein was much greater in the cytoplasm. We confirmed the distribution by transfecting the cells with a TTR construct that lacked the TTR leader sequence, which should result primarily in cytoplasmic distribution. That was the case, although there was also a weak TTR signal from the membrane containing fraction (results not shown). As expected, the production of TTR protein was markedly reduced in the cells bearing the leaderless construct. Hence in these cells wild type TTR was available to interact with C99 either in the cytoplasm or the cell membrane fraction containing the endoplasmic reticulum and endosomal compartments. When we examined the lysates using an antibody for phosphorylated threonine 668, only the membrane-associated fraction gave a detectable signal, a finding consistent with prior data regarding the cellular site of phosphorylation [35] (Fig.4).

What are the consequences of TTR binding to C99?

In order to determine whether the interaction of TTR with AβPP and C99 had any impact on Aβ production we measured the amount of Aβ in the culture medium of the three cell types after overnight incubation. Figure 5 shows that media from Aβ-producing CHO and SH-SY5Y cells transfected with the pcDNA-TTR constructs contained considerably less Aβ than identical cultures transfected with pcDNA-LacZ (SH-SY5Y reduced by 25%; 7PA2, 7WD10 reduced by 60%). There was no detectable loss of metabolic activity in any of the cell lines as measured by the resazurin assay, hence the reduction in Aβ secretion did not reflect a toxic effect of the transfected constructs (not shown) [36]. The amounts of Aβ-ELISA positive material in the cell lysates were not significantly different in the presence of TTR (Fig 5B), suggesting that the differences in the Aβ concentration in the media reflected a reduced rate of production of the secreted Aβ. The amounts of secreted sAβPPβ appeared to be comparable in the media of both *TTR* and *lacZ* transfected CHO cells (Fig. 5C).

Does TTR binding affect phosphorylation of AβPP and C99 at T668?

Since TTR binding to C99 appears to involve T668 we examined whether phosphorylation of that threonine was reduced in the pcDNA-TTR transfected cells. In the transfected 7PA2 AβPP-expressing CHO cells bearing the TTR cDNA the proportion of threonine 668-phosphorylated C99 (pC99), as detected by an antibody specific for phosphorylated threonine 668 (pT668), was reduced by approximately one third relative to that in the cells transfected with pcDNA-LacZ but there is no reduction in the proportion of pAPP (Figure 6 and Table 1). A similar result was observed comparing pcDNA-LacZ and pcDNA-TTR transfected SH-SY5Y human neuroblastoma cells, i.e. the proportion of pC99 was lower in the TTR transfected cells (Figure 7). We obtained the same result in the presence of the gamma secretase inhibitor DAPT [30].

Does TTR have the same effects on AβPP processing in APP23 mice *in vivo*?

Brains from age (13 mos.) and gender (male) matched APP23 mice in which the wild type human *TTR* gene is over-expressed and APP23 mice with intact *Ttr* genes were extracted and the relative amounts of pT668 and unphosphorylated forms of APP related peptides were compared by western blotting using the pT668 specific antibodies(figure 8)[3]. The relative amounts of phosphorylated and unphosphorylated AβPP and C99 derived from figure 8 are shown in Table 2. The amounts of AβPP and C99 are reduced in the TTR expressing mice. While the amount of pC99 is lower in the TTR mice it is proportional to the reduction in total C99. Similarly the reduction in pAPP is reduced to the same extent as the total amount of APP.

Discussion

Prior studies have suggested, somewhat counter-intuitively, that the human systemic amyloid precursor TTR plays a role in neuronal resistance to AD [1,2,37,38]. In humans 70% of neurons in AD brains stained with an anti-TTR antibody (compared with 10% in age matched non-demented controls) [3] and when examined in the context of the well-validated APP23 transgenic model of Aβ deposition in which over-expression of the human wild type *TTR* gene suppressed the associated neuropathologic and behavioral abnormalities. Thus in this setting, TTR plays a role in neuronal defense [5]. The mechanism responsible for the salutary effect of TTR appeared to be detoxification of Aβ by its interaction with oligomers and fibrils and the prevention of oligomerization by binding of the Aβ monomer [3,16]. However, immunochemical analyses of SDS and formic acid extractable $A\beta_{1\text{-}40}$ and $A\beta_{1\text{-}42}$ from brains of APP23-wt h*TTR* transgenics revealed that the amyloidogenic peptides were reduced [by 60–75% (SDS); 50–55% (formic acid)], suggesting decreased production of the aggregation prone peptides, rapid clearance in Aβ-TTR complexes, or some combination of the two. The current data confirm the *in vivo* observation indicating that Aβ formation is decreased in the presence of TTR. In the aggregate the data suggest a mechanism whereby TTR behaves as a multimodal suppressor of AD pathogenesis, inhibiting the production of the amyloidogenic precursor, “chaperoning” Aβ monomers, preventing the formation of cytotoxic oligomers and binding to oligomers and fibrils.

It has been suggested in other contexts that therapeutic approaches to neurodegenerative diseases resulting from protein aggregation might include reducing the expression of the precursor, or in the case of AD reducing the production of the amyloidogenic fragments by inhibiting secretase activity, promoting the binding of the aggregation precursor to chaperone-like molecules, reducing post-translational modifications that effect generation of the precursors, stabilizing monomers or very small oligomers in a pre-toxic state or enhancing aggregation to generate large non-toxic non-tissue damaging polymeric forms [39]. It appears that the naturally occurring neuronally synthesized TTR has many of these properties. The current studies revealed that in a model membrane environment [21] recombinant wt hTTR interacted with recombinant C99 causing major shifts in NMR peaks of the C99 residues G659 (APP_{695} numbering), A665 and T668. Titration of the interaction with each residue yielded binding curves indicating stoichiometric complex formation characterized by a single K_d. The three affected amino acids reside in the 35 residue

cytoplasmic loop anchored to the membrane. Thus the binding site is either exposed to cytoplasmic TTR (Fig 9) or the interaction occurs prior to insertion of the precursor molecule into the membrane, which seems less likely.

TTR is primarily a secreted protein, transiting the ER and Golgi prior to release into the medium. The fact that the C99 binding site is on the cytoplasmic portion of membrane raised the issue of whether there was cytoplasmic TTR available to access residues G659, A665 and T668. In studies examining the phenomenon of pre-emptive quality control HEK293 cells were transfected with a wild type TTR construct then subjected to ER stress (thapsigargin or MG132) [40–42]. The TTR protein was found in the cytoplasm with an intact leader sequence, similar to what we have seen in the 7PA2 cells transfected with either the wild type or leaderless TTR constructs (fig.4). Hence in these cells, the production of Aβ and its oligomers appears to constitute sufficient ER stress to result in the retro-translocation or cytoplasmic retention of TTR, making it available to interact with the cytoplasmic portion of C99. Thus under these circumstances TTR is found in the cytoplasm as well as in the membrane delimited ER.

Since phosphorylation of T668 is thought to impact AβPP processing, we examined T668 phosphorylation of AβPP and C99 in the presence of TTR. Western blots using antibodies to C99 and phospho-threonine 668 (pT668) suggested that all the AβPP-producing cultured cells (7PA2, WD10, SH-SY5Y) transfected with an efficiently transcribed and translated wt-hTTR construct had lower levels of phosphorylated C99 than cells transfected with pcLacZ. The variation in results among the cell lines may reflect differences in their kinase profiles [43–46]. We did not demonstrate significant differences in phosphorylation of T668 in full length AβPP in the presence of TTR. This was surprising since we assumed that AβPP would be phosphorylated prior to processing and phosphorylated AβPP was readily seen in both the cultured cells and the brain extracts. Thus it is possible that TTR can only access T668 after BACE cleavage of AβPP. This would suggest, intriguingly, that T668 accessibility to the TTR homo-tetramer differs between C99 and full length AβPP, perhaps because full length AβPP, but not C99, is homo-dimeric under cellular conditions [47]. Studies of cells transfected with a C50 construct encoding the C99 protein showed that T668 was readily phosphorylated in the absence of the AβPP ectoplasmic domain [48]. Alternatively it may be that failure to demonstrate an effect on phosphorylation of T668 in intact AβPP is a function of the small proportion of AβPP (10–20% or less depending on the state of differentiation of the neurons) that is normally phosphorylated [48,49]. Since only a fraction of total AβPP, all of it unphosphorylated, co-immunoprecipitated with TTR after cross-linking, it might be difficult to see a small difference.

When we compared cerebral cortical lysates from age and gender matched APP23 AD model mice and animals also overexpressing a wt h*TTR* transgene the western blots indicated that the levels of both AβPP and C99 were lower in the human TTR over-expressing mice (Table 2). While we found a profound reduction in formic acid and SDS soluble Aβ1-40 and Aβ1-42 in our prior experiments, we did not observe an overall reduction in APP and C99, perhaps because we did not rigorously match the animals for age and gender as we have done here (5). Since both APP and C99 concentrations were proportionately reduced and we did not see a similar effect in the transfected cells the

explanation may be technical rather than biologic, although we cannot eliminate a neuron-specific effect of TTR on APP expression *in vivo* not seen in the cultured stably APP-transfected CHO cells or that the interaction between TTR and AβPP seen in figure 3 reduces the amount of precursor protein [48].

It is also possible that TTR reduces Aβ production by a mechanism unrelated to its effect on phosphorylation. Binding C99 at a site encompassing T668 could alter γ-secretase recognition of C99, disabling cleavage with subsequent reduction in the amount of Aβ secreted into the media. Blocking access of γ-secretase to its cleavage site has also been proposed to explain the effect of BRI2 protein on Aβ production [50].

The significance of the phosphorylation at T668 is unclear. It has been argued that it regulates the γ-secretase cleavage responsible for generating the amyloidogenic Aβ fragments [51,52]. In these studies we demonstrate that co-expression of TTR in a culture system that robustly produces pathogenic Aβ fragments reduces the concentration of these fragments in the culture medium by 60 per cent. Whether that is related to its effect on phosphorylation or an effect on the conformation of the transmembrane domain of C99 that undergoes γ-secretase cleavage or both could not be distinguished in our experiments. Nonetheless in principle these studies, coupled with our prior observations, provide several mechanisms possibly responsible for the salutary effect of over-expression of the wild type human *TTR* gene in the APP23 model of human Aβ deposition.

The data also provide further insight into the functions of TTR as a binding molecule with conformational specificity. Although the TTR amino acids involved in the interaction with C99 are located in and around its T4 binding site, they are not those previously found to show resonance shifts on binding the Aβ monomer *in vitro* (Figs 1 and 2) [16]. Amino acid M13 appeared to be involved in both C99 and Aβ binding. While V16 was clearly involved in the Aβ interaction, its shift on exposure to C99 was less certain. The findings suggest that the TTR “T4 binding site” defines a hydrophobic region formed by the TTR tetramer that is capable of interacting with small molecules including and resembling thyroxine (T4), peptides, and regions of larger proteins via hydrophobic interactions [16,29,53]. The specificity of the interaction with a particular ligand is a function of individual amino acids within that conformational space (Table 3). In contrast to T4, which TTR binds with nanomolar K_d, binding of C99 is of modest affinity (K_d on the order of 85 μM). Notably the Aβ residues reacting with TTR (amino acids 17–21) are situated in the hydrophobic core of the $Aβ_{1-40/42}$ amyloidogenic peptide. Similarly the interactive C99 residues are located in the central portion of its cytoplasmic loop in which 6 of the 10 amino acids are hydrophobic (compared to the flanking ten residues closer to the membrane on either side, each of which contains only two hydrophobic amino acids). These observations support the notion that the hydrophobic region of TTR comprising the T4 binding site can interact with hydrophobic segments of peptides as well as small molecules such as thyroxine and the TTR amyloid therapeutic tafamidis, the conformational space behaving as a “zip code” or “area code” and the specific amino acids as an address or phone number.

Thus the beneficial *in vivo* effect of over-expression of a wild type human *TTR* gene in the APP23 model of human Aβ deposition can be explained by the capacity of the protein to

both inhibit Aβ aggregation and toxicity and reduce the production of potentially amyloidogenic fragments via an effect on γ-secretase cleavage. The multiplicity of molecular mechanisms involving TTR interactions with Aβ peptides and their precursor may explain why TTR expression is increased in seventy per cent of neurons in the human AD brain. It is known that the concentration of TTR in the serum of humans and mice decreases with aging but there are no data available documenting an alteration in neuronal TTR production with increasing age [54,55]. It has previously been suggested that neuronal HSF1 responses, primarily measured in terms of HSP70, are reduced in aged mice but recent data suggest that may not be the case [56,57]. If neuronal TTR production is diminished in aging, whether it reflects reduced HSF1 responsiveness or not, its reduction could contribute to the association of sporadic neurodegenerative disease with age.

Acknowledgments

W.M. Keck foundation (JB, XL); NIH grant RO1 GM106672 (CS); The NMR instrumentation at Vanderbilt used in this work was supported by NIH grant S10 RR025677-01 and by NSF grant DBI-0922862.

Reference List

1. Schwarzman AL, Goldgaber D. Interaction of transthyretin with amyloid beta-protein: binding and inhibition of amyloid formation. Book chapter, *Ciba Found Symp*. 1996; 199:146–160.
2. Stein TD, Johnson JA. Lack of neurodegeneration in transgenic mice overexpressing mutant amyloid precursor protein is associated with increased levels of transthyretin and the activation of cell survival pathways. J Neurosci. 2002; 22:7380–7388. [PubMed: 12196559]
3. Li X, Masliah E, Reixach N, Buxbaum JN. Neuronal production of transthyretin in human and murine Alzheimer's disease: is it protective? J Neurosci. 2011; 31:12483–12490. [PubMed: 21880910]
4. Wang X, Cattaneo F, Ryno L, Hulleman J, Reixach N, Buxbaum JN. The Systemic Amyloid Precursor Transthyretin (TTR) Behaves as a Neuronal Stress Protein Regulated by HSF1 in SH-SY5Y Human Neuroblastoma Cells and APP23 Alzheimer's Disease Model Mice. J Neurosci. 2014; 34:7253–7265. [PubMed: 24849358]
5. Buxbaum JN, Ye Z, Reixach N, Friske L, Levy C, Das P, Golde T, Masliah E, Roberts AR, Bartfai T. Transthyretin protects Alzheimer's mice from the behavioral and biochemical effects of Abeta toxicity. Proc Natl Acad Sci USA. 2008; 105:2681–2686. [PubMed: 18272491]
6. Stein TD, Anders NJ, Decarli C, Chan SL, Mattson MP, Johnson JA. Neutralization of transthyretin reverses the neuroprotective effects of secreted amyloid precursor protein (APP) in APPSW mice resulting in tau phosphorylation and loss of hippocampal neurons: support for the amyloid hypothesis. J Neurosci. 2004; 24:7707–7717. [PubMed: 15342738]
7. Brouillette J, Caillierez R, Zommer N, Alves-Pires C, Benilova I, Blum D, De SB, Buee L. Neurotoxicity and Memory Deficits Induced by Soluble Low-Molecular-Weight Amyloid-beta1-42 Oligomers Are Revealed In Vivo by Using a Novel Animal Model. J Neurosci. 2012; 32:7852–7861. [PubMed: 22674261]
8. Choi SH, Leight SN, Lee VM, Li T, Wong PC, Johnson JA, Saraiva MJ, Sisodia SS. Accelerated Abeta deposition in APPswe/PS1deltaE9 mice with hemizygous deletions of TTR (transthyretin). J Neurosci. 2007; 27:7006–7010. [PubMed: 17596449]
9. Doggui S, Brouillette J, Chabot JG, Farso M, Quirion R. Possible Involvement of Transthyretin in Hippocampal beta-Amyloid Burden and Learning Behaviors in a Mouse Model of Alzheimer's Disease (TgCRND8). Neurodegener Dis. 2010; 7:88–95. [PubMed: 20173334]
10. Wati H, Kawarabayashi T, Matsubara E, Kasai A, Hirasawa T, Kubota T, Harigaya Y, Shoji M, Maeda S. Transthyretin accelerates vascular Abeta deposition in a mouse model of Alzheimer's disease. Brain Pathol. 2009; 19:48–57. [PubMed: 18429966]

11. Schwarzman AL, Tsiper M, Wente H, Wang A, Vitek MP, Vasiliev V, Goldgaber D. Amyloidogenic and anti-amyloidogenic properties of recombinant transthyretin variants. Amyloid. 2004; 11:1–9. [PubMed: 15185492]
12. Costa R, Goncalves A, Saraiva MJ, Cardoso I. Transthyretin binding to A-Beta peptide -Impact on A-Beta fibrillogenesis and toxicity. FEBS Lett. 2008; 582:936–942. [PubMed: 18295603]
13. Du J, Murphy RM. Characterization of the interaction of beta-amyloid with transthyretin monomers and tetramers. Biochem. 2010; 49:8276–8289. [PubMed: 20795734]
14. Liu L, Murphy RM. Kinetics of inhibition of beta-amyloid aggregation by transthyretin. Biochem. 2006; 45:15702–15709. [PubMed: 17176092]
15. Giunta S, Valli MB, Galeazzi R, Fattoretti P, Corder EH, Galeazzi L. Transthyretin inhibition of amyloid beta aggregation and toxicity. Clin Biochem. 2005; 38:1112–1119. [PubMed: 16183049]
16. Li X, Zhang X, Ladiwala A, Du D, Yadav J, Tessier P, Wright P, Kelly J, Buxbaum J. Mechanisms of Transthyretin Inhibition of beta-Amyloid Aggregation In Vitro. J Neurosci. 2013; 33:19423–19433. [PubMed: 24336709]
17. Philibert KD, Marr RA, Norstrom EM, Glucksman MJ. Identification and characterization of Abeta peptide interactors in Alzheimer's disease by structural approaches. Front Aging Neurosci. 2014; 6:265. [PubMed: 25346686]
18. Cascella R, Conti S, Mannini B, Li X, Buxbaum JN, Tiribilli B, Chiti F, Cecchi C. Transthyretin suppresses the toxicity of oligomers formed by misfolded proteins in vitro. Biochim Biophys Acta. 2013; 1832:2302–2314. [PubMed: 24075940]
19. Mannini B, Cascella R, Zampagni M, van Waarde-Verhagen M, Meehan S, Roodveldt C, Campioni S, Boninsegna M, Penco A, Relini A, Kampinga HH, Dobson CM, Wilson MR, Cecchi C, Chiti F. Molecular mechanisms used by chaperones to reduce the toxicity of aberrant protein oligomers. Proc Natl Acad Sci USA. 2012; 109:12479–12484. [PubMed: 22802614]
20. Nhan HS, Chiang K, Koo EH. The multifaceted nature of amyloid precursor protein and its proteolytic fragments: friends and foes. Acta Neuropathologica. 2015; 129:1–19. [PubMed: 25287911]
21. Barrett PJ, Song Y, Van Horn WD, Hustedt EJ, Schafer JM, Hadziselimovic A, Beel AJ, Sanders CR. The amyloid precursor protein has a flexible transmembrane domain and binds cholesterol. Science. 2012; 336:1168–1171. [PubMed: 22654059]
22. Beel AJ, Mobley CK, Kim HJ, Tian F, Hadziselimovic A, Jap B, Prestegard JH, Sanders CR. Structural studies of the transmembrane C-terminal domain of the amyloid precursor protein (APP): does APP function as a cholesterol sensor? Biochem. 2008; 47:9428–9446. [PubMed: 18702528]
23. Podlisny MB, Ostaszewski BL, Squazzo SL, Koo EH, Rydell RE, Teplow DB, Selkoe DJ. Aggregation of secreted amyloid beta-protein into sodium dodecyl sulfate-stable oligomers in cell culture. J Biol Chem. 1995; 270:9564–9570. [PubMed: 7721886]
24. Zuurendonk PF, Tager JM. Rapid separation of particulate components and soluble cytoplasm of isolated rat-liver cells. Biochimica et Biophysica Acta. 1974; 333:393–399. [PubMed: 19400050]
25. Brocks DG, Siess EA, Wieland OH. Validity of the digitonin method for metabolite compartmentation in isolated hepatocytes. Biochem J. 1980; 188:207–212. [PubMed: 7406879]
26. McCarthy FM, Burgess SC, van den Berg BH, Koter MD, Pharr GT. Differential detergent fractionation for non-electrophoretic eukaryote cell proteomics. J Proteome Res. 2005; 4:316–324. [PubMed: 15822906]
27. Song Y, Hustedt EJ, Brandon S, Sanders CR. Competition between homodimerization and cholesterol binding to the C99 domain of the amyloid precursor protein. Biochem. 2013; 52:5051–5064. [PubMed: 23865807]
28. Lim KH, Dyson HJ, Kelly JW, Wright PE. Localized Structural Fluctuations Promote Amyloidogenic Conformations in Transthyretin. J Mol Biol. 2013
29. Alhamadsheh MM, Connelly S, Cho A, Reixach N, Powers ET, Pan DW, Wilson IA, Kelly JW, Graef IA. Potent kinetic stabilizers that prevent transthyretin-mediated cardiomyocyte proteotoxicity. Sci Translat Med. 2011; 3 97ra81.
30. Dovey HF, John V, Anderson JP, Chen LZ, de Saint AP, Fang LY, Freedman SB, Folmer B, Goldbach E, Holsztynska EJ, Hu KL, Johnson-Wood KL, Kennedy SL, Kholodenko D, Knops JE,

Latimer LH, Lee M, Liao Z, Lieberburg IM, Motter RN, Mutter LC, Nietz J, Quinn KP, Sacchi KL, Seubert PA, Shopp GM, Thorsett ED, Tung JS, Wu J, Yang S, Yin CT, Schenk DB, May PC, Altstiel LD, Bender MH, Boggs LN, Britton TC, Clemens JC, Czilli DL, Dieckman-McGinty DK, Droste JJ, Fuson KS, Gitter BD, Hyslop PA, Johnstone EM, Li WY, Little SP, Mabry TE, Miller FD, Audia JE. Functional gamma-secretase inhibitors reduce beta-amyloid peptide levels in brain. J Neurochem. 2001; 76:173–181. [PubMed: 11145990]

31. Lomant AJ, Fairbanks G. Chemical probes of extended biological structures: synthesis and properties of the cleavable protein cross-linking reagent [35S]dithiobis(succinimidyl propionate). J Mol Biol. 1976; 104:243–261. [PubMed: 957432]
32. Vassar R. beta-Secretase, APP and Abeta in Alzheimer's disease. Subcell Biochem. 2005; 38:79–103. [PubMed: 15709474]
33. Wolfe MS. Processive proteolysis by gamma-secretase and the mechanism of Alzheimer's disease. Biol Chem. 2012; 393:899–905. [PubMed: 22944690]
34. Nizard P, Tetley S, le DY, Watrin T, le GP, Wilson MR, Michel D. Stress-induced retrotranslocation of clusterin/ApoJ into the cytosol. Traffic. 2007; 8:554–565. [PubMed: 17451556]
35. Lee MS, Kao SC, Lemere CA, Xia W, Tseng HC, Zhou Y, Neve R, Ahlijanian MK, Tsai LH. APP processing is regulated by cytoplasmic phosphorylation. J Cell Biol. 2003; 163:83–95. [PubMed: 14557249]
36. Rampersad SN. Multiple applications of Alamar Blue as an indicator of metabolic function and cellular health in cell viability bioassays. Sensors. 2012; 12:12347–12360. [PubMed: 23112716]
37. Serot JM, Christmann D, Dubost T, Couturier M. Cerebrospinal fluid transthyretin: aging and late onset Alzheimer's disease. J Neurol Neurosurg Psychiatry. 1997; 63:506–508. [PubMed: 9343132]
38. Link CD. Expression of human beta-amyloid peptide in transgenic Caenorhabditis elegans. Proc Natl Acad Sci USA. 1995; 92:9368–9372. [PubMed: 7568134]
39. Lashuel HA, Overk CR, Oueslati A, Masliah E. The many faces of alpha-synuclein: from structure and toxicity to therapeutic target. Nat Rev Neurosci. 2013; 14:38–48. [PubMed: 23254192]
40. Rane NS, Kang SW, Chakrabarti O, Feigenbaum L, Hegde RS. Reduced translocation of nascent prion protein during ER stress contributes to neurodegeneration. Develop Cell. 2008; 15:359–370.
41. Kang SW, Rane NS, Kim SJ, Garrison JL, Taunton J, Hegde RS. Substrate-specific translocational attenuation during ER stress defines a pre-emptive quality control pathway. Cell. 2006; 127:999–1013. [PubMed: 17129784]
42. Kadowaki H, Nagai A, Maruyama T, Takami Y, Satrimafitrah P, Kato H, Honda A, Hatta T, Natsume T, Sato T, Kai H, Ichijo H, Nishitoh H. Pre-emptive Quality Control Protects the ER from Protein Overload via the Proximity of ERAD Components and SRP. Cell Rep. 2015; 13:944–956. [PubMed: 26565908]
43. Suzuki T, Oishi M, Marshak DR, Czernik AJ, Nairn AC, Greengard P. Cell cycle-dependent regulation of the phosphorylation and metabolism of the Alzheimer amyloid precursor protein. EMBO J. 1994; 13:1114–1122. [PubMed: 8131745]
44. Aplin AE, Gibb GM, Jacobsen JS, Gallo JM, Anderton BH. In vitro phosphorylation of the cytoplasmic domain of the amyloid precursor protein by glycogen synthase kinase-3beta. J Neurochem. 1996; 67:699–707. [PubMed: 8764598]
45. Iijima K, Ando K, Takeda S, Satoh Y, Seki T, Itohara S, Greengard P, Kirino Y, Nairn AC, Suzuki T. Neuron-specific phosphorylation of Alzheimer's beta-amyloid precursor protein by cyclin-dependent kinase 5. J Neurochem. 2000; 75:1085–1091. [PubMed: 10936190]
46. Standen CL, Brownlees J, Grierson AJ, Kesavapany S, Lau KF, McLoughlin DM, Miller CC. Phosphorylation of thr(668) in the cytoplasmic domain of the Alzheimer's disease amyloid precursor protein by stress-activated protein kinase 1b (Jun N-terminal kinase-3). J Neurochem. 2001; 76:316–320. [PubMed: 11146006]
47. Jung JI, Premraj S, Cruz PE, Ladd TB, Kwak Y, Koo EH, Felsenstein KM, Golde TE, Ran Y. Independent relationship between amyloid precursor protein (APP) dimerization and gamma-secretase processivity. Plos ONE. 2014; 9:e111553. [PubMed: 25350374]
48. Chang KA, Kim HS, Ha TY, Ha JW, Shin KY, Jeong YH, Lee JP, Park CH, Kim S, Baik TK, Suh YH. Phosphorylation of amyloid precursor protein (APP) at Thr668 regulates the nuclear

translocation of the APP intracellular domain and induces neurodegeneration. Molec Cell Biol. 2006; 26:4327–4338. [PubMed: 16705182]

49. Nakaya T, Suzuki T. Role of APP phosphorylation in FE65-dependent gene transactivation mediated by AICD. Molec Cell Mech. 2006; 11:633–645.
50. Matsuda S, Giliberto L, Matsuda Y, McGowan EM, D'Adamio L. BRI2 inhibits amyloid beta-peptide precursor protein processing by interfering with the docking of secretases to the substrate. J Neurosci. 2008; 28:8668–8676. [PubMed: 18753367]
51. Feyt C, Pierrot N, Tasiaux B, Van HJ, Kienlen-Campard P, Courtoy PJ, Octave JN. Phosphorylation of APP695 at Thr668 decreases gamma-cleavage and extracellular Abeta. Biochem Biophys Res Comm. 2007; 357:1004–1010. [PubMed: 17459339]
52. Vingtdeux V, Hamdane M, Gompel M, Begard S, Drobecq H, Ghestem A, Grosjean ME, Kostanjevecki V, Grognet P, Vanmechelen E, Buee L, Delacourte A, Sergeant N. Phosphorylation of amyloid precursor carboxy-terminal fragments enhances their processing by a gamma-secretase-dependent mechanism. Neurobiol Dis. 2005; 20:625–637. [PubMed: 15936948]
53. Baures PW, Oza VB, Peterson SA, Kelly JW. Synthesis and evaluation of inhibitors of transthyretin amyloid formation based on the non-steroidal anti-inflammatory drug, flufenamic acid. Bioorg Med Chem. 1999; 7:1339–1347. [PubMed: 10465408]
54. Buxbaum J, Koziol J, Connors LH. Serum transthyretin levels in senile systemic amyloidosis: effects of age, gender and ethnicity. Amyloid. 2008; 15:255–261. [PubMed: 19065297]
55. Teng MH, Yin JY, Vidal R, Ghiso J, Kumar A, Rabenou R, Shah A, Jacobson DR, Tagoe C, Gallo G, Buxbaum J. Amyloid and nonfibrillar deposits in mice transgenic for wild-type human transthyretin: a possible model for senile systemic amyloidosis. Lab Invest. 2001; 81:385–396. [PubMed: 11310831]
56. Tonkiss J, Calderwood SK. Regulation of heat shock gene transcription in neuronal cells. Int J Hyperthermia. 2005; 21:433–444. [PubMed: 16048840]
57. Carnemolla A, Labbadia JP, Lazell H, Neueder A, Moussaoui S, Bates GP. Contesting the dogma of an age-related heat shock response impairment: implications for cardiac-specific age-related disorders. Hum Molec Genet. 2014; 23:3641–3656. [PubMed: 24556212]

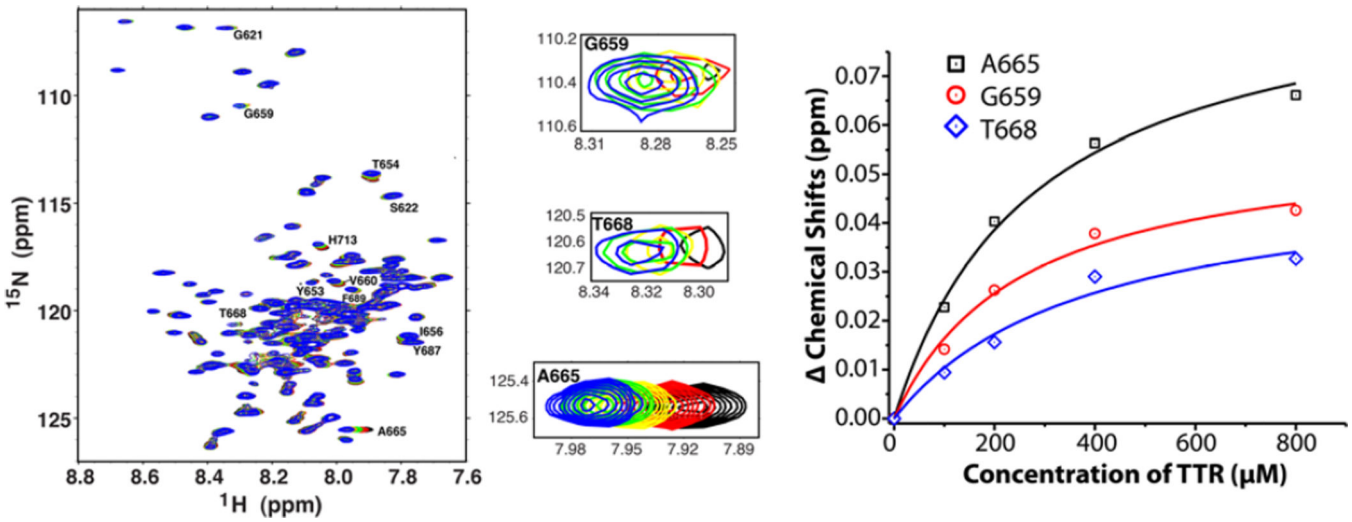

Figure 1. Nuclear magnetic resonance analysis of the titration of uniformly ^{15}N-labeled human C99 by wild type human TTR *in vitro*

The left and middle panels show the ^{1}H, ^{15}N-TROSY NMR spectra of uniformly-^{15}N-labeled C99 in LMPG micelles as a 250 μM solution of C99 was titrated with unlabeled TTR to the following concentrations: 0 (black), 100 μM (red), 200 μM (yellow), 400 μM (green), and 800 μM (blue). All solutions contained 5% (w/v) LMPG, 20 mM Na^{+}-phosphate, pH 7.2, and the spectra were collected at 900 MHz and 310K. Peak assignments are from (22). The right panel shows the chemical shift changes for the three indicated peaks as a function of TTR concentration. Alanine 665 (A665), Glycine 659 (G659) and Threonine 668 T668 are designated according to APP_{695} numbering. For each, the best fit of a 1:1 binding model to the data is shown, with the determined $_{D}$ given in the Results.

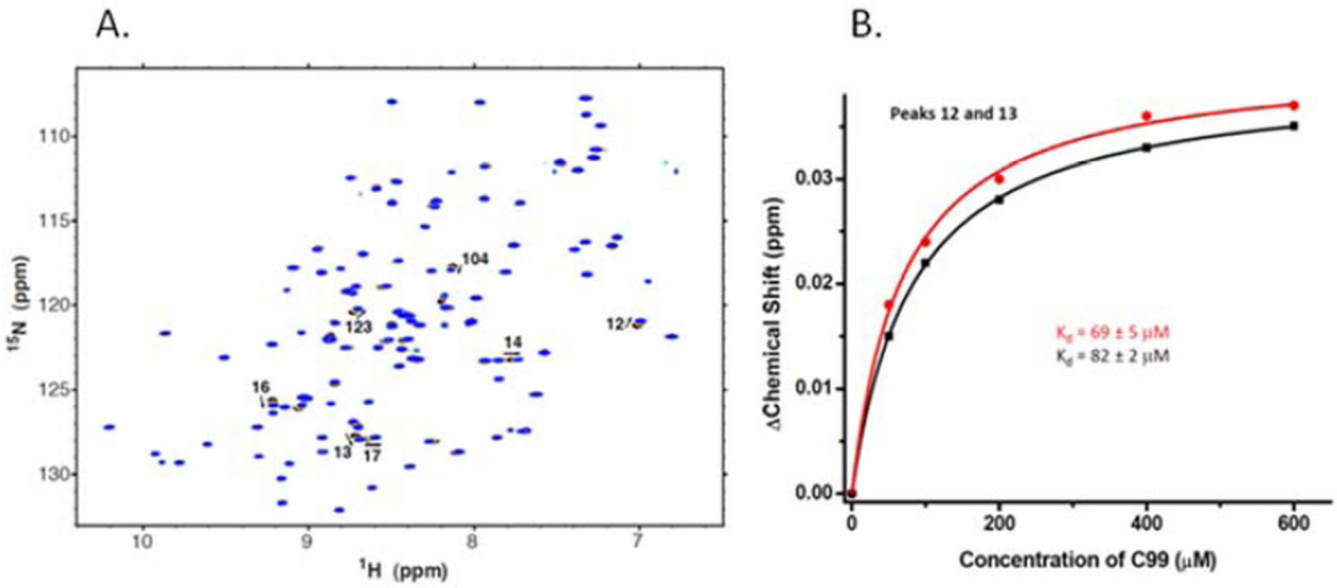

Figure 2. Nuclear magnetic resonance analysis of the titration of uniformly ^{15}N-labeled wild type TTR by C99 *in vitro*

A. ^{1}H, ^{15}N-TROSY NMR spectra of uniformly-^{15}N-labeled TTR as a 100 μM solution was titrated with unlabeled C99. All solutions contained 5% (w/v) LMPG, 100 mM Na^{+}-phosphate, pH 7.2, and the spectra were collected at 900 MHz and 310K. Indicated peak assignments are based on those reported in (28). B. ^{1}H, ^{15}N-TROSY NMR peak chemical shift changes for the two indicated peaks of uniformly ^{15}N-labeled TTR as it was titrated by unlabeled C99. For each, the best fit of a 1:1 binding model is shown, with the determined K_D as indicated.

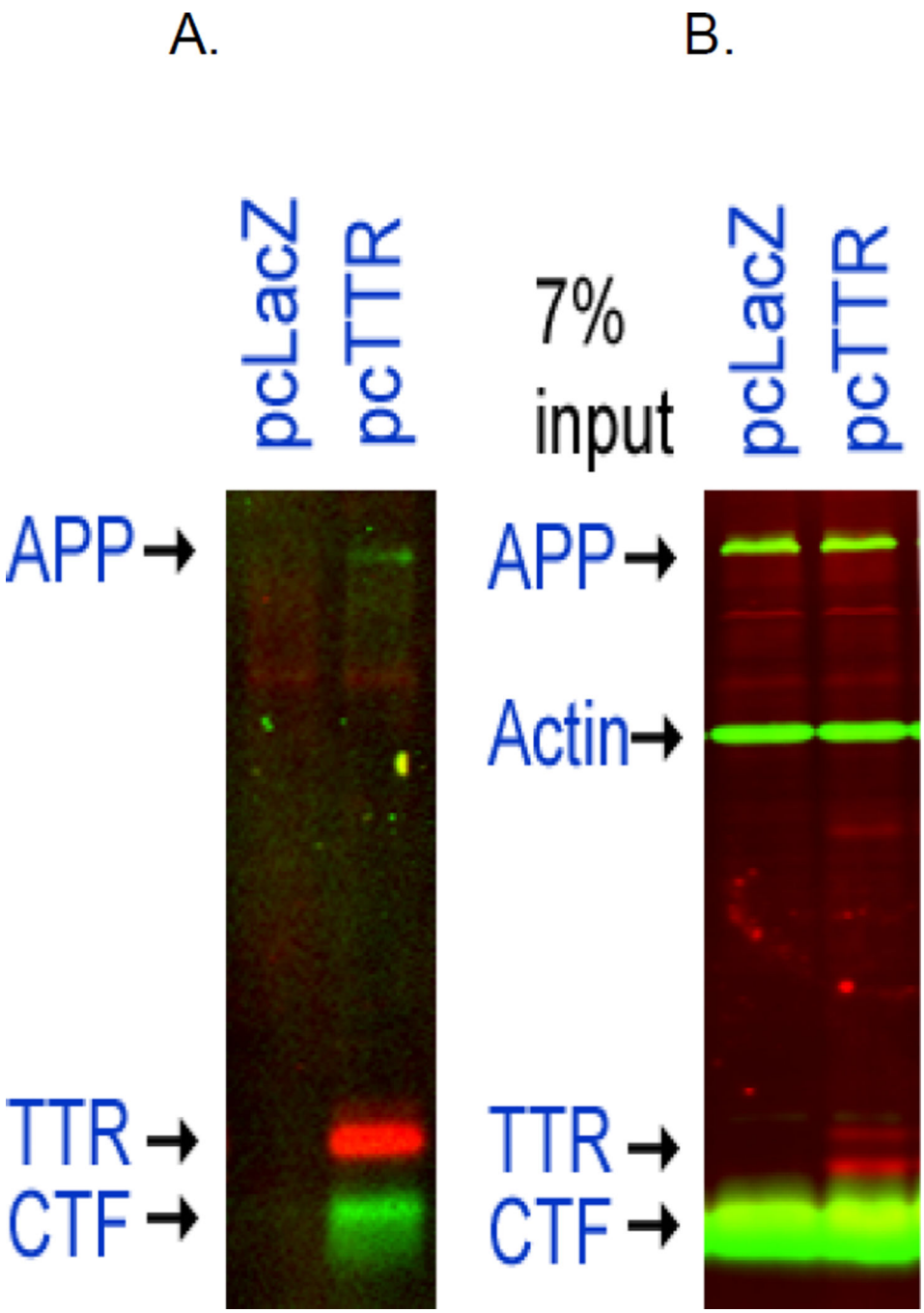

Figure 3. Immunoprecipitation of molecules cross-linked to TTR in 7PA2 ($APP_{Val717Phe}$) cells transfected with a wt hu TTR plasmid

The 7PA2 cells containing the two constructs were incubated overnight with 1μM DAPT to decrease digestion of CTF then lysed and the lysates analyzed by western blotting. Panel A shows that the anti-TTR antibody (DAKO,linked to Dynabeads) pulls down complexes that had been cross-linked intracellularly by the membrane permeable cross-linker DSP. The complexes contained TTR, CTF, APP proteins only from the 7PA2 cells expressing $APP_{Val717Phe}$ transfected with the pcDNA-TTR construct, not from cells transfected with the

control LacZ construct. Similar results were seen in 7WD10 cells which express wt AβPP (not shown). Panel B shows the lysate from which the immunoprecipitates were prepared.

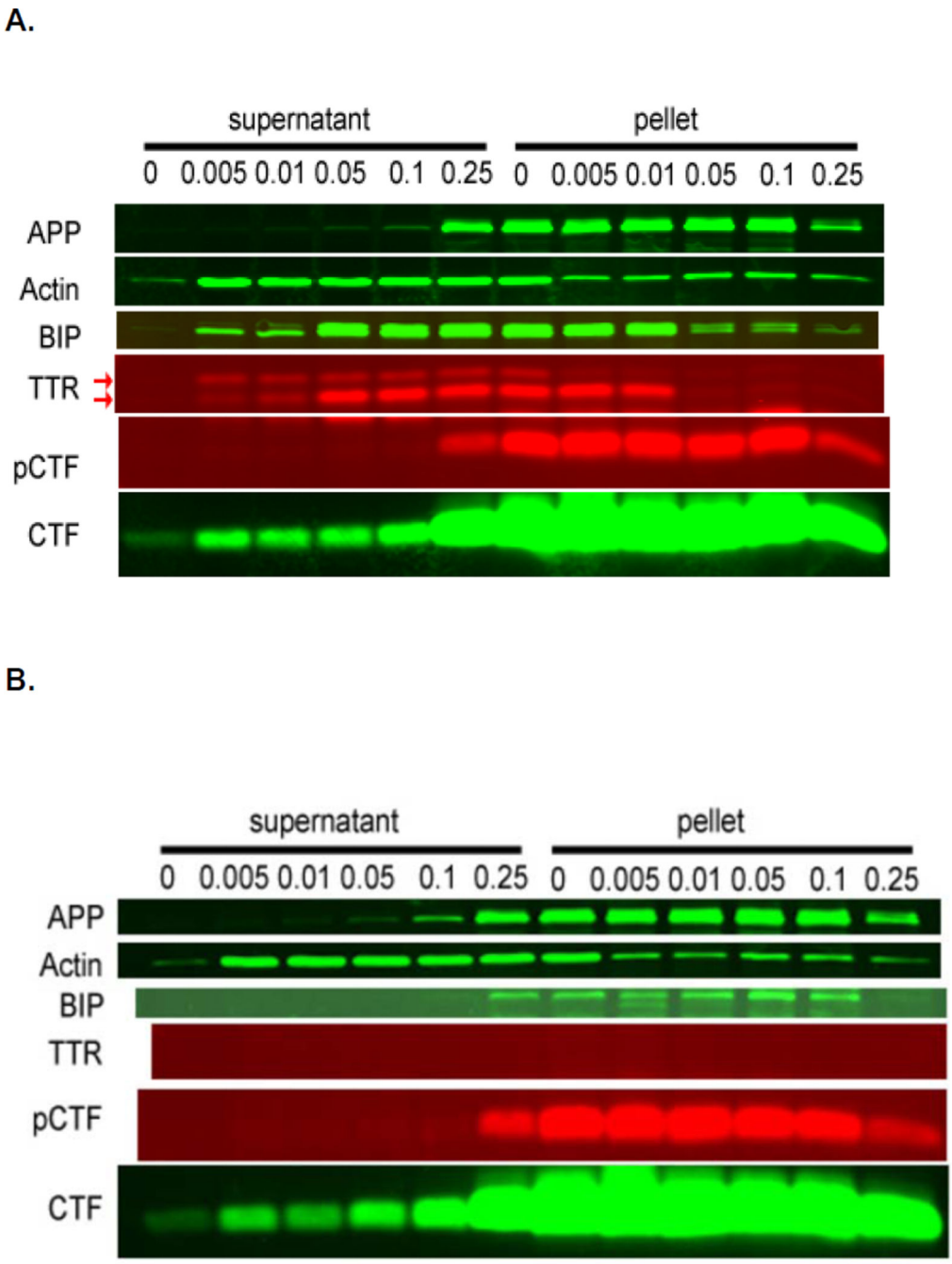

Figure 4. Digitonin fractionation of 7PA2 cells transfected with a human TTR containing plasmid (A) or the pLacZ control plasmid (B)

7PA2 cells expressing and processing the AD-associated $APP_{Val717Phe}$ variant transfected with the pcDNA-TTR and expressing wt huTTR were extracted with increasing concentrations of digitonin. Antibodies specific for the proteins identified on the left (see methods for specific antibodies) were used to develop western blots of the digitionin solubilized (supernatant) and insoluble fractions (pellet) as indicated. The supernatant fractions from cells treated with digitonin 0.005–0.1 % represent cytoplasmic extracts. 0.05–0.1 % represents cytoplasm and ER extracts. 0.25 % digitonin solubilizes membrane-

containing structures including the cytoplasm, ER and vesicles. Actin is a primarily cytoplasmic marker. BiP is a predominantly ER compartment marker. It is clear that APP, CTF and pCTF (T668 phosphorylated CTF) are all found in the membrane-containing fractions of each preparation. APP and pCTF (detected with antibody C1/61) are found only in the 0.25% digitonin fractions. The two bands stained with the anti-TTR serum identified by the arrows represent the protein with (upper band) and without (lower band) the leader sequence. The experiment was repeated three times. The data suggest that in the TTR transfected over-expressing cells both processed and unprocessed (retaining its “leader” sequence) TTR are retrotranslocated to the cytoplasm. The small proportion of BiP in the cytoplasmic fraction may represent ER damage but the relative amount of unprocessed TTR in the low digitionin fractions is much greater indicating active retrotranslocation of TTR rather than ER leakage. The distributions of the phosphorylated and unphosphorylated forms of the APP-related molecules were the same in control pLacZ transfected 7PA2 cells (without TTR) panel B.

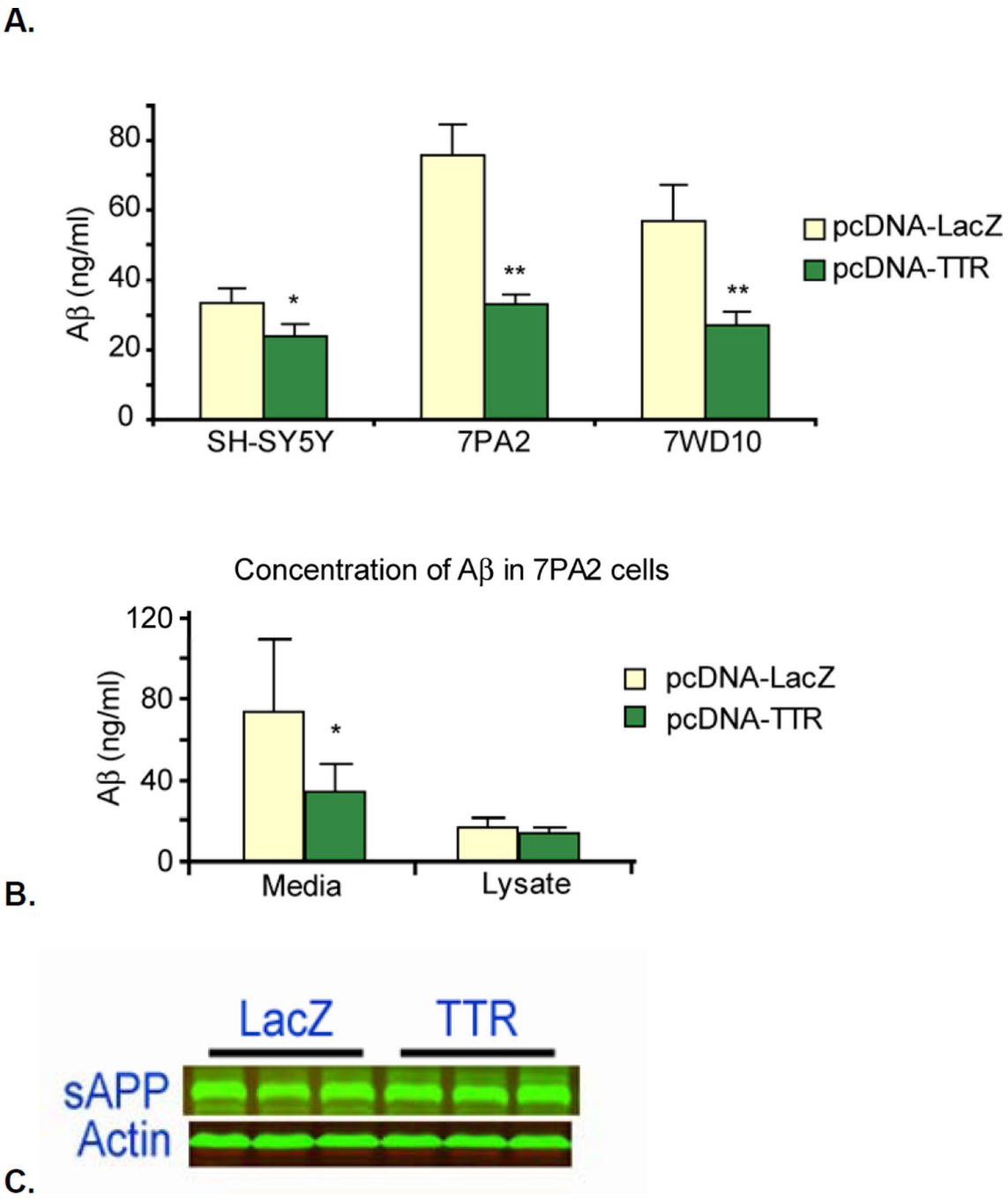

Figure 5. CHO cells expressing APP, i.e. 7PA2 ($APP_{Val717Phe}$), 7WD10 (wt APP), and SH-SY5Y cells transfected with pcDNA-LacZ and pcDNA-TTR

Panel A shows that the amount of Aβ protein as determined by ELISA is reduced in all the cell lines that also express human TTR. Panel B shows that while the amount of Aβ released into the media by the TTR-transfected 7PA2 cells was diminished, the amounts of Aβ in the cell lysates were similar in the presence and absence of TTR. The experiments with the 7PA2 and 7WD10 cells were repeated three times. The SH-SY5Y experiment was done only once. Panel C shows that the amounts of secreted sAPPβ (the product of BACE cleavage of

AβPP) were similar, suggesting that the effects of TTR were downstream of the generation of sAPPβ and C99 by BACE1.

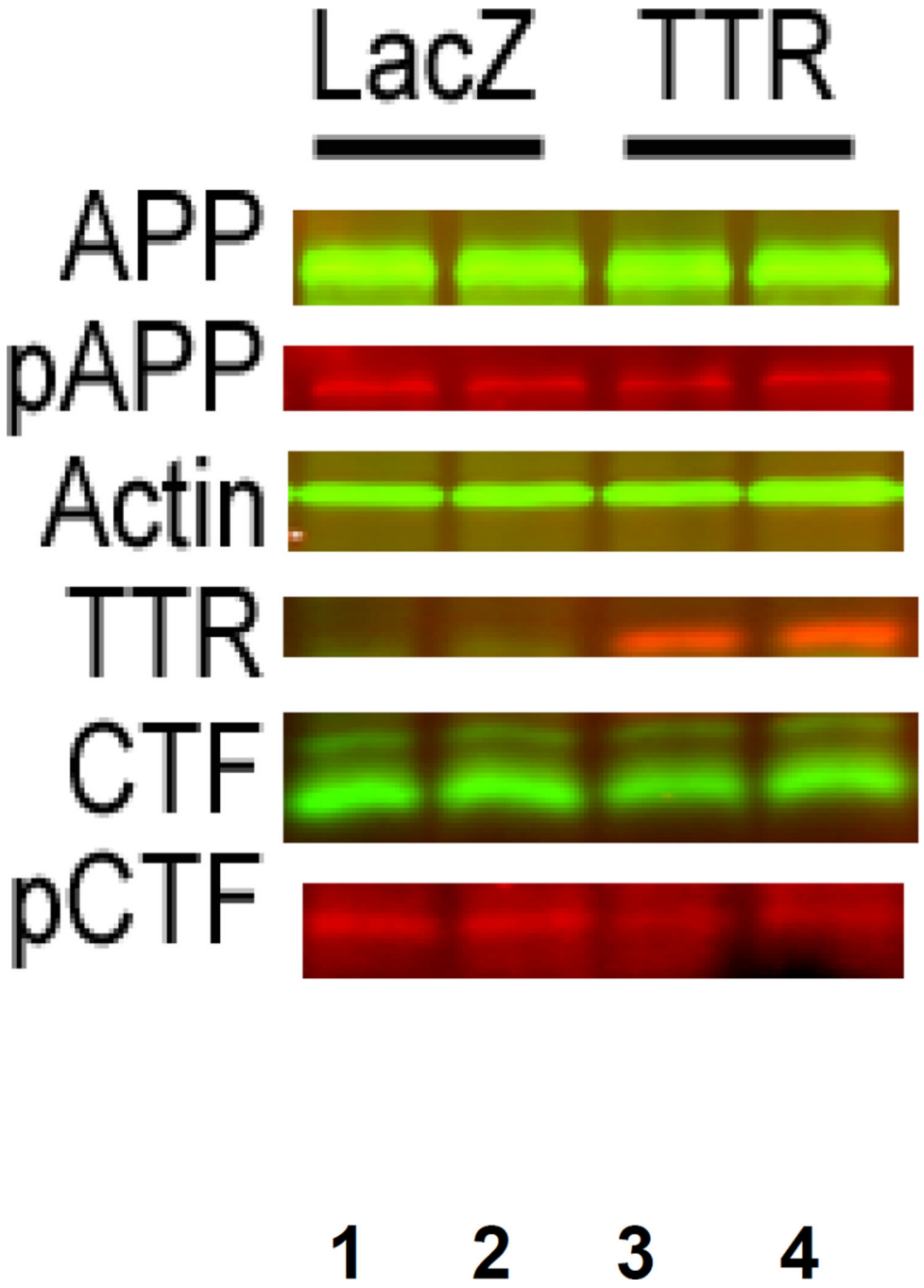

Figure 6. Differences in CTF Phosphorylation in 7PA2 cells transfected with either pcDNA-TTR or pcDNA-LacZ

Lanes 1 and 2 are from 7PA2 cells transfected with pcDNA-LacZ construct while 3 and 4 are from pcDNA-TTR transfectants. The calculated proportions of phosphorylated T668 in the treated cells are shown in Table 1.

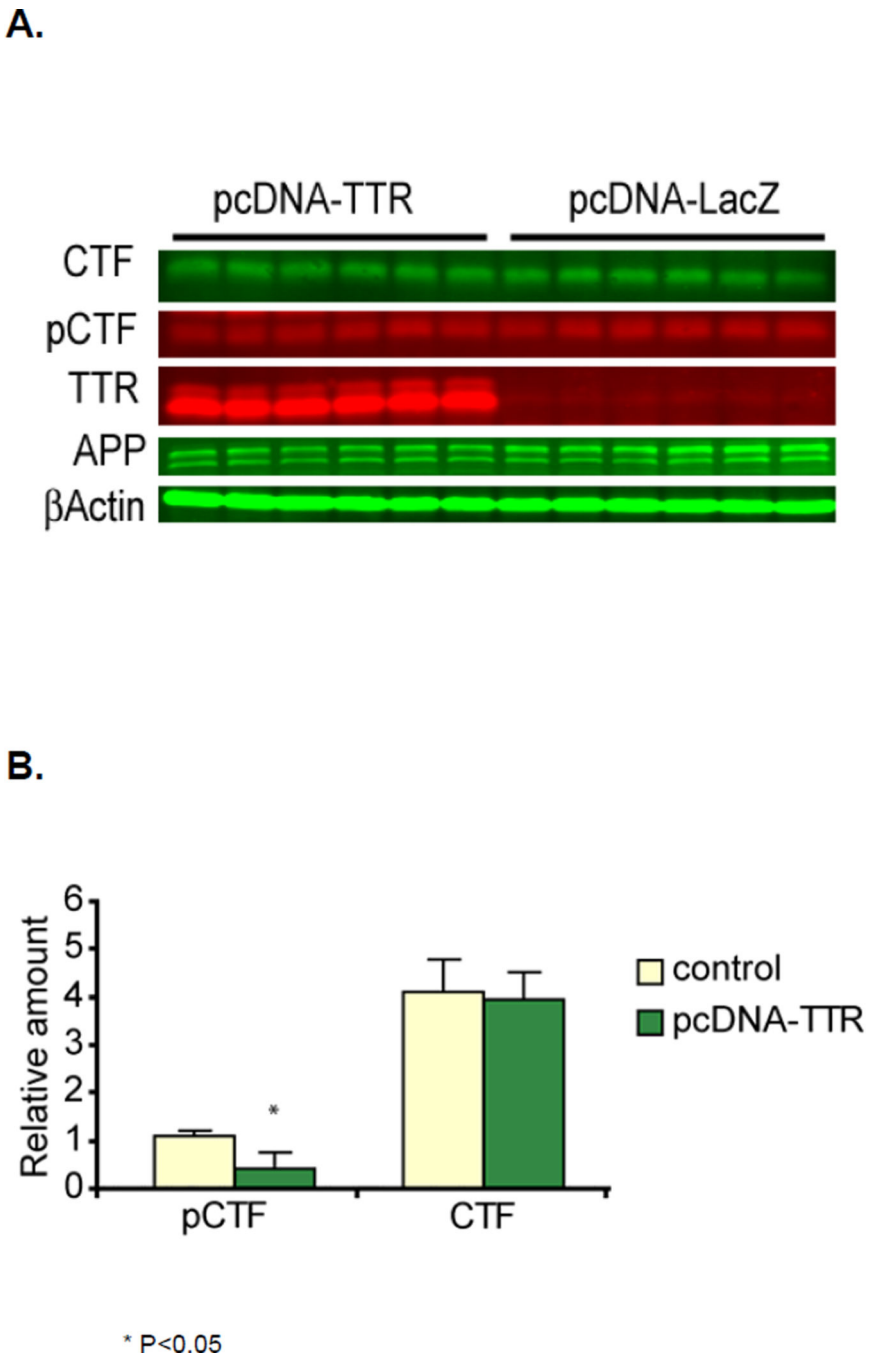

Figure 7. Comparison of relative amounts of phosphorylated CTF in SH-SY5Y cells transfected with pcDNA-TTR and pcDNA-LacZ in the presence of the gamma secretase inhibitor DAPT

Panel A. Western blots of SH-SY5Y human neuroblastoma cells transfected with either pcDNA-LacZ or pcDNA-TTR and probed with antibodies for AβPP (C1/61), TTR and phosphorylated T668. **Panel B** shows the quantitation, i.e. indicating a significantly lower degree of phosphorylation in cells transfected with the TTR-encoding plasmid. (*) indicates that the difference is significant with a p value of 0.05.

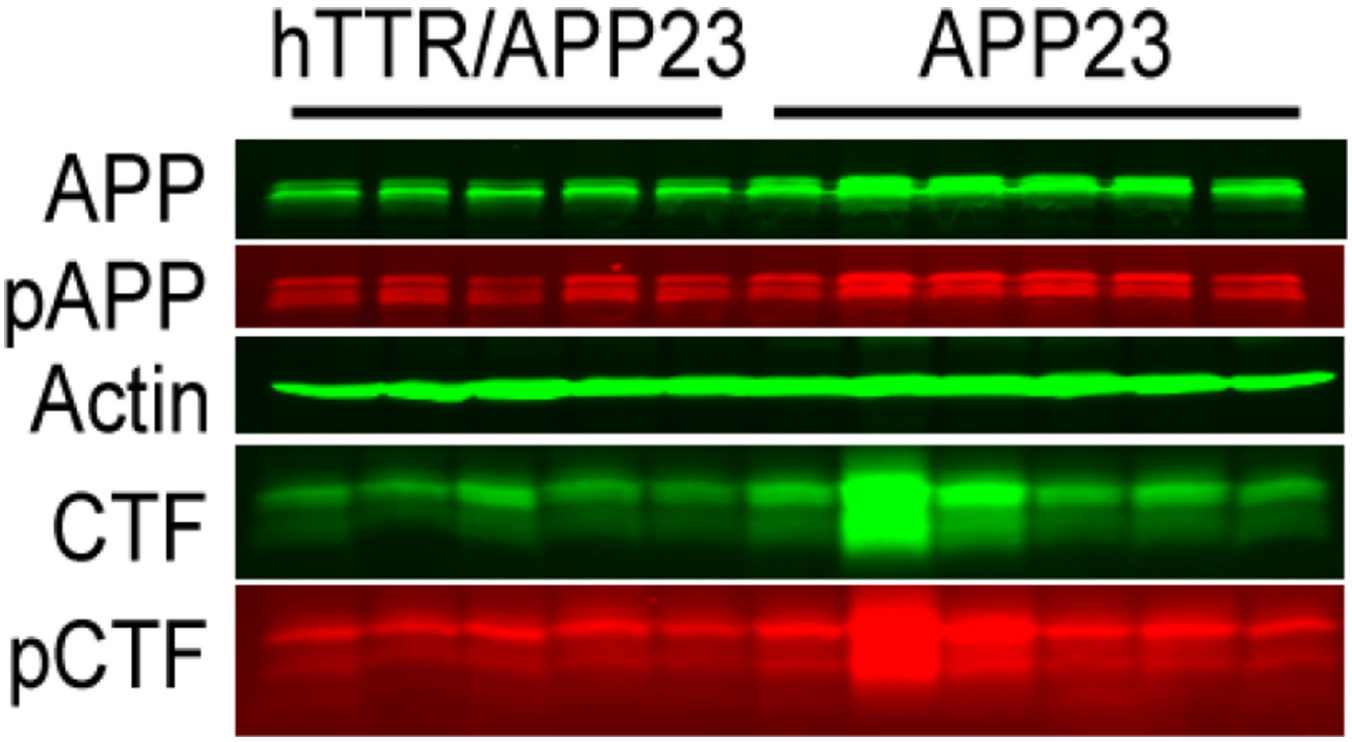

Figure 8. Western blots of extracts of brains from 13 month old male APP23 mice compared with those from age and gender matched APP23 mice over-expressing wild type human TTR developed with antibodies specific for AβPP peptides (C1/61) and phosphorylated T668

Western blots of brain extracts from age and gender matched transgenic mice expressing a human AD-associated Swedish APP mutation in the presence and absence of an over-expressed human TTR gene. The westerns were repeated three times with the results the same on each gel. For quantitation the proteins in each sample were normalized to the actin concentration. The relative proportion of each molecular species is quantified in Table 2.

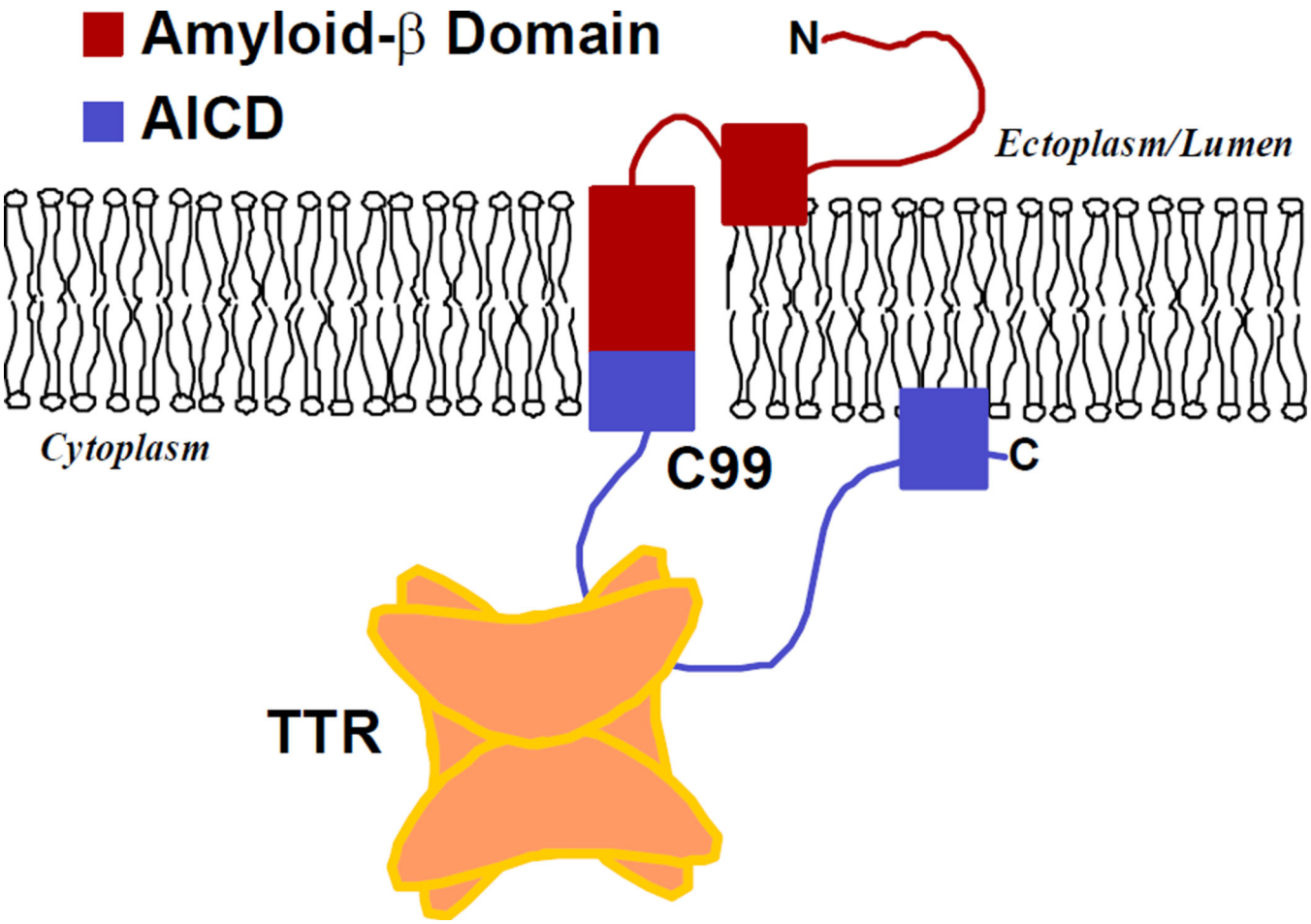

Figure 9. Model of the Interaction between transthyretin and the AβPP C99 fragment

Model of the Interaction between transthyretin and the AβPP C99 fragment depicting the site of interaction in the thyroxine binding pocket region of TTR.

Table 1

Relative amounts of phosphorylated CTF and APP in 7PA2 Cells transfected with human TTR encoding and LacZ containing plasmids (Fig. 6)

7PA2	C99	pC99	pAPP	APP
	Avg. S.D.	Avg. S.D.	Avg. S.D.	Avg. S.D.
pCDNA-TTR	42.2±2.3	0.44±0.04	2.06±0.45	47.3±6.5
pcDNA-lacZ	46.6±1.9	0.69±0.11	1.97±0.15	47.9±2.9
p-value	0.04	0.01	0.75	0.90

Table 2

Quantitation of phosphorylated and unphosphorylated APP and C99 in brain extracts of age and gender matched APP23 and hTTR/APP23 mice (Fig. 8)

Strain	pC99	C99	pAPP	APP
	Avg. S.D.	Avg. S.D.	Avg. S.D.	Avg. S.D.
APP/hTTR	4.3 ± 1.0	8.9 ± 2.9	7.2 ± 1.1	17.3 ±1.1
APP	7.4 ± 3.5	17.1 ±8.7	9.7 ± 1.4	29.1 ±4.1
p-value	0.09	0.08	0.01	0.0002

Table 3

Ligand Binding in the Thyroxine-binding Pocket of Transthyretin (TTR)

Property	**Small Molecules**		**Proteins**	
Molecule	Thyroxine (T4)	Tafamidis	$A\beta_{1\text{-}40/42}$	C99
Kd	15nM	2nM	24μM	85μM
Stoichiometry	1–2	1–2	1	1
TTR binding site	K15, L17, T106, A109, L110, T119, S117	K15, L17, E54, T106, A109, L110, S117, T119	K15, L17, A109, L110, A120, V121,V122,M13,V16, A19, N27	L12, M13, V14, V16, R104, v123